Multioctave midinfrared supercontinuum generation in suspended-core chalcogenide fibers

O. Mouawad,[1] J. Picot-Clémente,[1] F. Amrani,[1] C. Strutynski,[1] J. Fatome,[1] B. Kibler,[1] F. Désévédavy,[1] G. Gadret,[1] J.-C. Jules,[1] D. Deng,[2] Y. Ohishi,[2] and F. Smektala[1,*]

[1]*ICB, Laboratoire Interdisciplinaire Carnot de Bourgogne, UMR 6303 CNRS—Université de Bourgogne, 9 Av. Alain Savary, BP 47870, 21078 Dijon, France*

[2]*Research Center for Advanced Photon Technology, Toyota Technological Institute 2-12-1, Hisakata, Tempaku, Nagoya 468-8511, Japan*

**Corresponding author: frederic.smektala@u-bourgogne.fr*

Received February 14, 2014; revised March 26, 2014; accepted March 27, 2014; posted March 28, 2014 (Doc. ID 206309); published April 24, 2014

An As_2S_3 fiber-based supercontinuum source that covers 3500 nm, extending from near visible to the midinfrared, is successfully reported by using a 200-fs-pulsed pump with nJ-level energy at 2.5 μm. The main features of our fiber-based source are two-fold. On the one hand, a low-loss As_2S_3 microstructured optical fiber has been fabricated, with typical attenuation below 2 dB/m in the 1–4 μm wavelength range. On the other hand, a 20-mm-long microstructured fiber sample is sufficient to enable a spectral broadening, spreading from 0.6 to 4.1 μm in a 40 dB dynamic range.

OCIS codes: (060.2390) Fiber optics, infrared; (060.5295) Photonic crystal fibers; (190.4370) Nonlinear optics, fibers; (160.4330) Nonlinear optical materials; (160.2750) Glass and other amorphous materials; (060.2270) Fiber characterization.

http://dx.doi.org/10.1364/OL.39.002684

Expanding the wavelength range of supercontinua toward the midinfrared region is of high technological interest in numerous applications, such as spectroscopy, sensing, biology, metrology, or defense. However, exceeding the fused silica transparency limits beyond 2 μm remains a challenging task [1]. To this aim, several strategies and alternative materials have been proposed so as to push back the edges of supercontinuum (SC) sources still further in the midinfrared region. In particular, wider transmission windows and stronger nonlinear materials have been studied as an alternative to fused silica, such as tellurite [2,3], fluoride glasses [4,5], heavy oxides [6] or chalcogenide glasses [7–15]. Given their remarkable optical and chemical properties, chalcogenide-based materials have been found to be promising candidates. Indeed, depending on their chemical composition, the infrared transparency can exceed 10 μm, whereas the Kerr nonlinearity can be three orders of magnitude higher than standard fused silica [7]. This combination of both properties makes them particularly attractive for broadband midinfrared SC generation. However, chalcogenide glasses suffer from a large normal group velocity dispersion (GVD) in the infrared, which dramatically reduces the efficiency of SC expansion. Indeed, the zero-dispersion wavelength (ZDW) is commonly located far in the midinfrared and far from standard commercially available laser sources. For instance, the ZDW of sulfide glasses are usually located around 5 μm, which makes them challenging to pump in their anomalous dispersion regime. Therefore, a well-designed geometry is required to shift down the ZDW to lower wavelengths. To this aim, several scenarios have been considered such as waveguide design [8–10], tapering [11–13], and microstructured optical fibers (MOFs) [2,14,15], which give rise to record spectral expansions in the midinfrared [2,8–15]. In this Letter, we report the generation of a 3500-nm bandwidth SC in a 2-cm-long segment of a low loss As_2S_3 suspended core MOF. The fiber geometry was carefully designed for an efficient pumping close to its ZDW in the anomalous dispersion regime by means of an OPO delivering 200-fs pulses at an operating wavelength of 2.5 μm. To the best of our knowledge, this is the largest SC bandwidth generated in chalcogenide fibers.

In order to fabricate the MOF, commercially available high purity elemental precursors (S and As of 5N purity) were first used to prepare a glass rod. Nevertheless, their subsequent distillation remains mandatory since the sulphur powder is generally polluted by water and carbon, while the surface of metallic arsenic is polluted by oxides. Thus, starting products were subjected to thermal treatment under a vacuum inside a silica setup to get rid of their respective impurities. Sulphur is thus dried by heating for a few hours at 120°C under a dynamic vacuum. Simultaneously, the arsenic is heated for a few hours at the oxide sublimation temperature (290°C) [2]. At a later stage, the mixed batches are enclosed inside silica glassware prior to static distillation. By means of the static distillation process, the batch collected inside the silica synthesis ampoule is exempt of unsuitable carbon. Finally, the synthesis ampoule was sealed and placed inside a three zone melting rocking furnace. The ampoule was then heated up to the reaction temperature (700°C) and maintained at this stage for several hours (12 h). At such high temperature, the melt reagents interact to form the glass. Enforced by high volatility of sulfur, the ampoule was slowly heated to avoid its explosion. Finally, the silica ampoule containing the liquid batch was quenched in water. The obtained sulfide glass was subsequently annealed at the glass transition temperature ($Tg = 210°C$) for 12 h. A mechanical drilling technique was adopted to elaborate the glass preforms. Thanks to this original technique, a variety of geometrical designs conceived to achieve well controlled parameters (core size, holes positions, inner surface) were prepared [2,7]. Here, the preform geometry

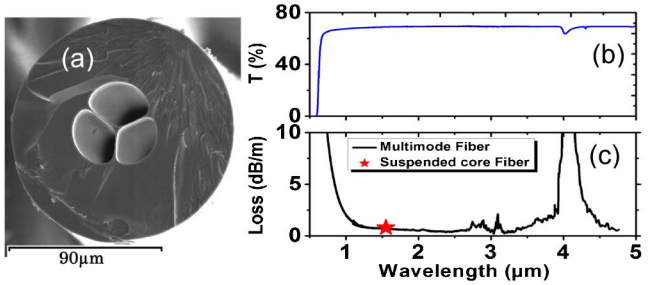

Fig. 1. (a) Profile of the chalcogenide As_2S_3 suspended-core fiber captured by means of scanning electronic microscopy, (b) chalcogenide bulk transmission, and (c) optical loss of the mono-index large core multimode fiber as a function of wavelength. Loss measured at 1.55 µm for the suspended core MOF (star).

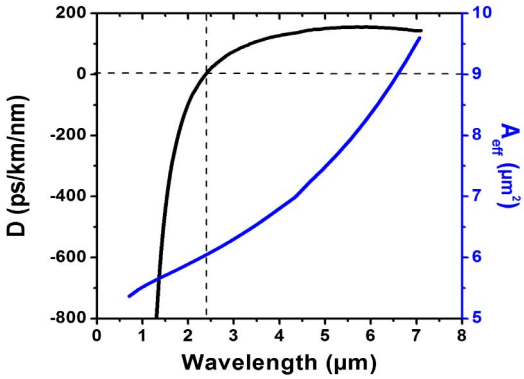

Fig. 2. Numerical modeling of the fundamental mode of the suspended-core chalcogenide fiber, showing the chromatic dispersion curve (upper, black curve) and effective mode area (lower, blue curve).

consists of three holes centered on a central solid core. The length of the fiber preform is 40 mm and the diameter of air holes is 1 mm. Following the drawing process, the fiber microstructure consists in a triangular lattice of air holes which extend along the fiber. They surround a small central core with triangle geometry attached to robust jacket by three thin struts. The corresponding cross-section image of the suspended core MOF is displayed in Fig. 1(a).

The fiber has an outer diameter of 130 µm and a central solid core of 3.4 µm in diameter, held to the clad through three surrounding holes by means of three thin struts. Due to technical constraints, the spectral losses cannot be directly measured on this resulting small core MOF. However, an estimation of fiber optical losses by means of a Fourier transformed infrared (FTIR) spectrometer can be performed on a mono-index large core multimode fiber [2]. Results are depicted in Figs. (1b) and (1c) in the range of 0.5–5 µm. In particular, we compare optical losses obtained from the chalcogenide bulk and the mono-index fiber. Two typical extrinsic absorption bands slightly emerge from the background. The first band is large and centered at 2.77 and 2.89 µm. This phenomenon is due to fundamental vibration modes of OH bonds. A second narrow band attributed to vibration mode of SH bonds is centered at 3.2 µm. The SH concentration level is quite high, above detection limits of our detection set-up (integrating sphere connected to an InSb detector) which explains the noisy aspect of the depicted spectrum and the lack of the SH absorption peak around its fundamental vibration wavelength at 4.0 µm. Taking advantage of the cut-back technique, and using a continuous wave laser source, we confirmed previous loss measurements for the suspended-core fiber at 1.55 µm [star in Fig. 1(c)]. However, in our previous work [2], we have suspected a dynamic time variation of the attenuation, especially related with OH absorption, which could be at the origin of limitation of the extension of the SC further in the infrared region. Thus, in order to confirm the aforementioned hypothesis, as well as to avoid any unsuitable variation of the attenuation of the fiber sample, the microstructured fiber freshly drawn has been permanently preserved under suitable conditions. Chalcogenide fibers were stored under anhydrous Nitrogen atmosphere inside a sealed box. This procedure allows us to control the moisture content of atmosphere at which the glass fibers are exposed and therefore to prevent the suspected aging process of As_2S_3 fibers.

Figure 2 reports numerical simulations of modal properties based on the fiber geometry derived from the SEM analysis [see Fig. 1(a)].

Our suspended core fiber exhibits a ZDW close to 2.4 µm. The core size mainly governs the fiber dispersion properties and it was chosen in such a way that the ZDW fits in the wavelength range of maximal power of the tunable mid-infrared laser source used below.

Figure 3 shows the experimental setup used for SC generation. It consists of an optical parametric oscillator (OPO) pumped by a Ti–sapphire laser. It generates tunable pulses extending from 1.7 up to 3.2 µm, with pulse width of 200 fs at a repetition rate of 80 MHz. The 2-cm-long sample of chalcogenide fiber is fixed onto a 3 axis holder. The incident beam is focused into the fiber using a midinfrared aspheric zinc selenide (ZnSe) focus lens with a numerical aperture (NA) of 0.25 at 3.2 µm. This setup allows us to pump the fiber under study on a wide range of wavelengths around its ZDW, so as to ensure an efficient SC generation [16]. The output SC is collected through a 0.5-m-long multimode fluoride (InF_3) fiber with high transmission over the 0.3–5.5 µm spectral range. It is then analyzed by means of two optical spectrum analyzers (OSAs) covering 350 to 1200 nm and 1200 to 2400 nm, respectively, as well as by a FTIR spectrometer in the range of 2.4 to 5 µm.

A series of *in situ* tests that evaluate the measured spectral broadening versus pump wavelength allowed us to select the suitable anomalous regime pump wavelength at 2.5 µm. From Fig. 2 we evaluated the GVD, β_2, to -0.06 ps^2 m^{-1}. The incoming average power was measured after the focusing lens, before being injected into the fiber. The maximum peak power available was 12 kW at an average power of 194 mW. Next, we measured the coupling coefficient of about 40% when using low input

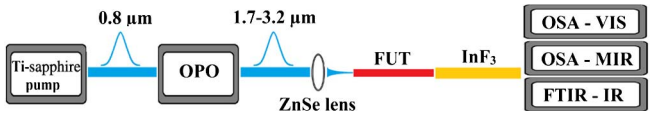

Fig. 3. Experimental setup used for SC generation in the suspended-core chalcogenide fiber. FUT, fiber under test.

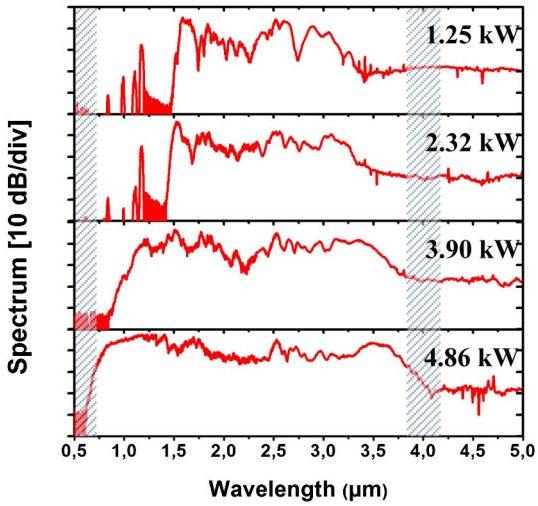

Fig. 4. Experimental recording of SC generation in a 20-mm-long sample of suspended-core chalcogenide fiber for pump peak power increasing from 1.25 to 4.86 kW. The main features of the As_2S_3 transmission window are also displayed by means of hashed areas, the glass band gap (hashed zone at 0.6 μm) and SH absorption band (hashed zone at 4.0 μm).

powers. Figure 4 shows the output spectra recorded for the tested fiber under a 2.5-μm pump wavelength according to injected peak power increasing from 1.25 to 4.86 kW. The nonlinear index of the material is $n_2 \sim 2.8 \times 10^{-18}$ $m^2\,W^{-1}$ at 1550 nm, which corresponds, from the 6.1 μm^2 effective mode area depicted in Fig. 2, to a nonlinear Kerr coefficient $\gamma = 1.15$ $W^{-1}\,m^{-1}$. The nonlinear length (L_{NL}) decreases from 0.7 to 0.18 mm when the input peak power is increased from 1.25 to 4.86 kW, respectively. Since the nonlinear length scale of this As_2S_3 MOF is estimated at below the millimeter range, according to the input pulse power, the large spectral broadening is expected to take place in the first millimeters of the MOF. For the highest peak power, the injected pulse corresponds to a high soliton number $N = 36$. The chalcogenide fiber is clearly pumped into the anomalous dispersion regime, and is characterized by a strong and rapid self-phase modulation process followed by soliton fission. Subsequent propagation is then associated with soliton dynamics and dispersive wave generation. Note that in this case the fission occurs randomly, due to the significant role of modulation instability when $N > 20$ [16], thus leading to significant degradation of SC coherence properties. The broadest resulting spectrum extends from 600 to 4100 nm in the −40 dB range, whereas the generated bandwidth at −20 dB covers from 700 to 3800 nm. Note that we outstandingly reached the glass transmission limit from the visible side, and no damage was reported on the MOF sample, even at maximum incoming power. Here, the corresponding output average power is ∼90% of the input power.

In our previous work [2], the output spectrum bandwidth was critically correlated to MOF attenuation, especially to OH and SH absorptions, whereas numerical simulations neglecting these dramatic absorption peaks revealed that dynamics of SC generation could be extended until 5.5 μm. Here, the control of aging combined with a gradual reduction of the length of the fiber sample under testing allows the issue of OH absorption to be overcome, but not completely that related to SH absorption. Hence, only 2 cm of fiber was used for this experiment to extend the SC long wavelength edge further to the MIR region. The broad spectrum cuts off in the MIR side at around 4.1 μm. It is primarily due to fiber attenuation, especially SH absorption around 4.0 μm. The signature of OH absorption can be observed using longer fiber segments, it depends at the same time on its concentration, its vibration modes, and the degree of OH hydrogen bonding present in the glass. The combination of different vibration modes (stretching and bending) of weekly H-bonded OH and free OH in the glass provide a 500 nm bandwidth absorption band located around 2.76 μm, spreading from 2.5 to 2.99 μm. Here, solitons successfully overcome these crucial absorptions and subsequently allow a better expansion of the spectrum in the MIR compared to our previous studies [2]. However, the impact of SH absorption at 4.0 μm appears for high input pulse power. Gradual increasing of the pump power allows for shifting the spectrum long wavelength edge further in the MIR region. However, note that the high SH absorption prevents here the efficient expansion of the spectral broadening beyond 4.1 μm.

In conclusion, we report here an As_2S_3 fiber-based SC source that covers 3500 nm, extending from the near visible to the midinfrared by using a 200-fs-pulsed pump with about 1 nJ energy at 2.5 μm. In particular, the SC bandwidth extends from the glass bandgap limit at 0.6 μm to the midinfrared region around 4.1 μm. To our knowledge, this is the largest SC bandwidth generated in chalcogenide fibers. The remaining limitation of the SC bandwidth is mainly related to the presence of the SH absorption peak. Additionally, we find that deleterious temporal evolution of the OH species of As_2S_3 MOF has been limited by the dry atmosphere storage technique, thus confirming the proposed aging hypothesis. A detailed study is in progress in order to discern the aging process and their inherent deleterious phenomena.

We acknowledge the financial support from the JSPS–CNRS Bilateral French–Japanese Program, the Conseil Régional de Bourgogne through the Photcom PARI program, as well as the French DGA. This project has been performed in cooperation with the Labex ACTION program (contract ANR-11-LABX-0001-01).

References

1. J. Hu, J. Meyer, K. Richardson, and L. Shah, Opt. Mater. Express **3**, 1571 (2013).
2. I. Savelii, O. Mouawad, J. Fatome, B. Kibler, F. Désévédavy, G. Gadret, J.-C. Jules, P.-Y. Bony, H. Kawashima, W. Gao, T. Kohoutek, T. Suzuki, Y. Ohishi, and F. Smektala, Opt. Express **20**, 27083 (2012).
3. P. Domachuk, N. A. Wolchover, M. Cronin-Golomb, A. Wang, A. K. George, C. M. B. Cordeiro, J. C. Knight, and F. G. Omenetto, Opt. Express **16**, 7161 (2008).
4. F. Théberge, J.-F. Daigle, D. Vincent, P. Mathieu, J. Fortin, B. E. Schmidt, N. Thiré, and F. Légaré, Opt. Lett. **38**, 4683 (2013).
5. G. Qin, X. Yan, C. Kito, M. Liao, C. Chaudhari, T. Suzuki, and Y. Ohishi, Appl. Phys. Lett. **95**, 161103 (2009).
6. J. H. V. Price, T. M. Monro, H. Ebendorff-Heidepreim, F. Poletti, P. Horak, V. Finazzi, Y. Y. Leong, P. Petropolis,

J. C. Flanagan, G. Brambilla, X. Feng, and D. J. Richardson, IEEE J. Sel. Top. Quantum Electron. **13**, 738 (2007).
7. J. Fatome, C. Fortier, T. N. Nguyen, T. Chartier, F. Smektala, K. Messaad, B. Kibler, S. Pitois, G. Gadret, C. Finot, J. Troles, F. Desevedavy, P. Houizot, G. Renversez, L. Brilland, and N. Traynor, J. Lightwave Technol. **27**, 1707 (2009).
8. Y. Yu, X. Gai, T. Wang, P. Ma, R. Wang, Z. Yang, D.-Y. Choi, S. Madden, and B. Luther-Davies, Opt. Mater. Express **3**, 1075 (2013).
9. M. R. E. Lamont, B. Luther-Davies, D. Y. Choi, S. Madden, and B. J. Eggleton, Opt. Express **16**, 14938 (2008).
10. J. McCarthy, H. Bookey, S. Beecher, R. Lamb, I. Elder, and A. K. Kar, Appl. Phys. Lett. **103**, 151103 (2013).
11. A. Al-kadry, C. Baker, M. El Amraoui, Y. Messaddeq, and M. Rochette, Opt. Lett. **38**, 1185 (2013).
12. S. Shabahang, G. Tao, J. J. Kaufman, and A. F. Abouraddy, J. Opt. Soc. Am. B **30**, 2498 (2013).
13. C. W. Rudy, A. Marandi, K. L. Vodopyanov, and R. L. Byer, Opt. Lett. **38**, 2865 (2013).
14. J. Hu, C. R. Menyuk, L. B. Shaw, J. S. Sanghera, and I. D. Aggarwal, Opt. Lett. **35**, 2907 (2010).
15. W. Gao, M. E. Amraoui, M. Liao, H. Kawashima, Z. Duan, D. Deng, T. Cheng, T. Suzuki, Y. Messaddeq, and Y. Ohishi, Opt. Express **21**, 9573 (2013).
16. J. M. Dudley, G. Genty, and S. Coen, Rev. Mod. Phys. **78**, 1135 (2006).